A Reflectarray Antenna Designed with Gain Filtering and Low-RCS Properties

Mei, Peng; Zhang, Shuai; Cai, Yang; Lin, Xianqi; Pedersen, Gert Frølund

Published in:
I E E E Transactions on Antennas and Propagation

DOI (link to publication from Publisher):
10.1109/TAP.2019.2911342

Publication date:
2019

Document Version
Accepted author manuscript, peer reviewed version

A Reflectarray Antenna Designed with Gain Filtering and Low RCS Properties

Peng Mei, *Student Member, IEEE*, Shuai Zhang, *Senior Member, IEEE*, Yang Cai, Xian Qi Lin, *Senior Member, IEEE*, and Gert Frølund Pedersen, *Senior Member, IEEE*

***Abstract*—This paper presents a reflectarray (RA) antenna operating at X-band with gain filtering and low radar cross section (RCS) properties. The unit cell (UC) for the proposed RA antenna design combines a band-notched absorber unit and a dielectric lens unit together, where the dielectric lens unit serving as a phase shift is coated on the absorber unit to achieve co-design. Importantly, it is required that the UCs should still maintain the high notch-band-edge selectivity property that the band-notched absorber originally has when the profile of the dielectric lens unit is varied to cover a full phase-cycle (2π) for the proposed RA antenna design. For demonstration, an absorber is presented with a high notch-band-edge selectivity and a wide absorption bandwidth performance in vertical and horizontal polarization, respectively; a dielectric lens based on square posts is rigorously designed to be coated on the absorber seamlessly to construct the desired UC. The simulated results show that the proposed RA antenna has a bandpass-like gain filtering performance and pencil-beam radiation patterns within the notch band, which is experimentally verified by the measured results. In addition, the measured results also reveal the RCSs of the proposed RA antenna are reduced significantly compared to counterparts of the conventional RA antenna in horizontal polarization and out of the notch band in vertical polarization.**

***Index Terms*—Reflectarray (RA) antenna, absorbing media, dielectric lens, phase shift, high gain, gain filtering, low RCS.**

I. Introduction

THE REFLECTARRAY (RA) antenna is composed of a quasi-periodic set of unit elements mostly set in a regular lattice to emulate a specific phase-front transformation [1], [2]. RA antennas have successfully found many areas requiring high-gain applications in place of classical parabola antennas or phased array antennas. The functions of RA antennas are fully developed in the past decades. The operating band(s) was extended from single-band to dual-band [3]-[8]; the operating polarization was improved from linearly polarized to circularly polarized [9]-[13], and so on. To accommodate the versatile wireless communications, the reconfigurable RA antennas were emerged to achieve various radiation performances by electronically or mechanically controlling phase responses of individual elements of the RA [14]-[17]. In [18], [19], RA antennas integrated with solar cells were reported to reduce the occupied area for different space and civilian applications [20]-[22]. The integrated RA antenna not only could have good radiation performance but also owe significant solar energy efficiency [18]. In [23], the authors utilized the perforated substrate to construct a broadband RA antenna. It was experimentally demonstrated that a 1-dB gain bandwidth of 29.5% was achievable while its out-of-band RCS can be reduced. The authors in [24] employed the tightly coupled dipole element to achieve an ultra-wide-band RA antenna with a bandwidth ratio of 3.12:1. To eliminate the conductor or dielectric loss, the pure metal or pure dielectric is served as the element structure to construct RA antennas [25], [26]. However, they usually suffer from a relatively bulky volume. To expand the function of an RA antenna, a technical point could be considered that the radar cross section (RCS) of an RA antenna should be significantly reduced out of the operating band.

In our previous literature [27], a band-notched absorber with high notch-band-edge selectivity was described. The notch band was generated by introducing two different resonances within a wide absorption band. The proposed band-notched absorber was also successfully assembled with a dipole antenna to achieve low radar cross section (RCS) [28], where the notch band was equivalently served as a necessary metal ground for the dipole antenna. It is found that the band-notched absorber unit had good potential to be employed to build an RA antenna with gain filtering and low-RCS properties. However, it is extremely difficult to maintain the high notch-band-edge selectivity of the absorber when the dimensions of the band-notched absorber unit are modified to cover a full phase-cycle (2π). In [29], the authors presented a methodology to control the reflection phase response from a 3-D bandstop structure backed with an absorbing material, where the reflection phase response of the structure within the reflection band is flexibly controlled by top-loaded metallic patches with variable size. As a result, a high gain and low radar cross section

Manuscript received Nov, 2018. This work was supported in part by National Natural Science Foundation of China under Grant 61571084, in part by EPRF under Grant 6141B06120101, in part by NDSTI under Grant 1716313ZT00802902, and in part by AAU Young Talent Program. (*Corresponding author: Shuai Zhang*)

P. Mei, S. Zhang, and G. F. Pedersen are all with the Antennas, Propagation and Millimeter-wave Systems section, Department of Electronic Systems, Aalborg University, Aalborg, 9220, Denmark. (email: sz@es.aau.dk)

Y. Cai and X. Q. Lin are all with the EHF Key Laboratory of Science, School of Electronic Science and Engineering, University of Electronic Science and Technology of China, Chengdu, 611731, China. X. Q. Lin is also with the Jiangsu Henxin Technology Co., Ltd, Wuxi, 214222, China. (email: xqlin@uestc.edu.cn)

RA antenna can be achieved based on the proposed methodology. However, it is found that when the size of the metallic patch is varied to satisfy a full phase-cycle (2π), the notch-band-edge selectivity of the UC is significantly degraded, which deteriorates the RCS reduction capability out of the stopband.

In this paper, a reflectarray antenna with bandpass-like gain filtering and low-RCS properties is investigated in detail. We construct a new unit cell (UC) by fully employing a band-notched absorber unit and a dielectric lens unit, where the dielectric lens unit is coated on the band-notched absorber, serving as a phase shifter. It is required that the extra addition of the dielectric lens should not only achieve a full phase-cycle but also maintain the high notch-band-edge selectivity that the original band-notched absorber has. For demonstration, a band-notched absorber with a high notch- band-edge selectivity in vertical polarization and a wide absorption bandwidth in horizontal polarization is presented for a linearly polarized RA antenna application. The dielectric lens based on square posts is optimized as the phase shifter, coated on the band-notched absorber to construct the proposed new UC for achieving co-design. The simulated results demonstrate that the high notch-band-edge selectivity of the proposed UC is still maintained when the profile of the dielectric lens unit is varied to cover a full phase-cycle. Based on the UCs, the proposed RA antenna operating at X-band is then constructed, simulated, fabricated, and measured. The simulated and measured results demonstrate that the proposed RA antenna has a bandpass-like gain filtering and pencil-beam radiation within the notch band from 9.0 to 10.5 GHz, which are experimentally proved by the measured results. In addition, the measured results also reveal that the proposed RA antenna has great RCS reductions out of the notch band from 7 to 9.2 GHz in the lower band and from 10.5 to 13 GHz in the upper band (corresponding to the fractional bandwidth of 27.16 % and 21.27 %, respectively) and a wideband RCS reduction from 7 to 13 GHz (with a fractional bandwidth of 60 %) in horizontal polarization compared to the counterparts of a conventional RA antenna.

The outlines of the paper are organized as follows: in section II, the procedures to achieve the proposed UC are described in detail; section III presents the implementation of the proposed RA antenna using the proposed UCs; in section IV, the proposed RA antenna is fabricated, and its radiation patterns, realized gains, and monostatic RCS are measured and discussed; some remarkable conclusions are summarized in section V.

II. Unit Cell Design

A. Absorber with a high notch-band-edge selectivity in vertical polarization and a wide absorption bandwidth in horizontal polarization.

In this subsection, a band-notched absorber is designed with a polarization-discrimination performance that it shows a high notch-band- edge selectivity in vertical polarization, and a wide absorption bandwidth in horizontal polarization.

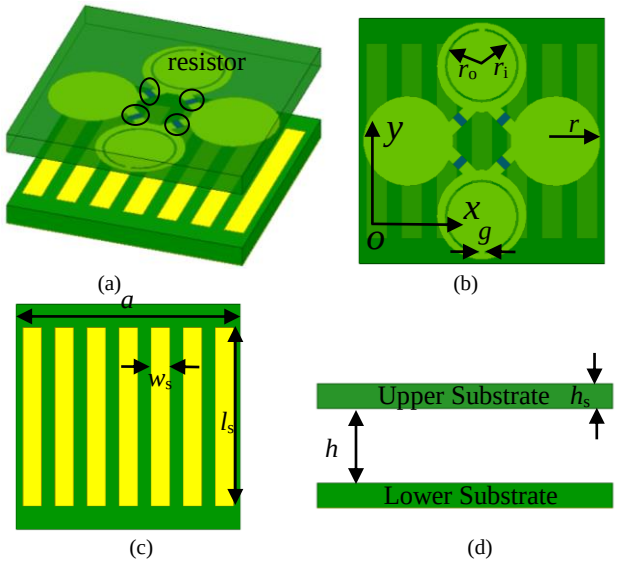

Fig.1. Geometries of the band-notched absorber unit. (a) Perspective view. (b) Front view of the upper layer. (c) Front view of the lower layer. (d) Side view. (a=12.0 mm, hs=1.0 mm, l_s=10.5 mm, w_s=1.0 mm, r=2.2 mm, r_i=1.7 mm, r_o=1.8 mm, g=0.3 mm, h=3.0 mm)

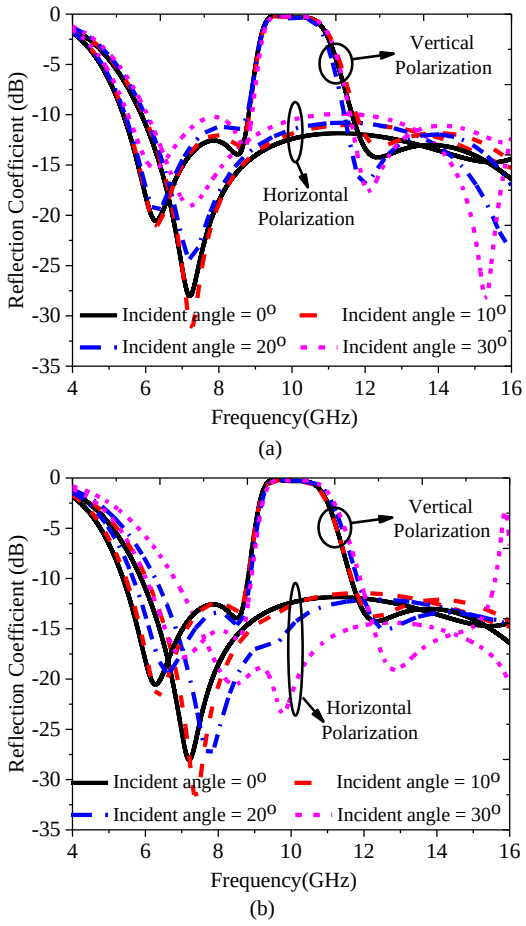

Fig.2. Reflection coefficients of the proposed absorber under normal and oblique incidences in vertical and horizontal polarization. (a) TE-wave, (b) TM-wave.

This article has been accepted for publication in a future issue of this journal, but has not been fully edited. Content may change prior to final publication. Citation information: DOI 10.1109/TAP.2019.2911342, IEEE Transactions on Antennas and Propagation

Fig. 1 presents the geometries of the proposed absorber unit cell. It consists of two pairs of circular dipole-shaped metal strips in orthogonal position printed on the upper supporting substrate, a metallic rectangular strip array printed on the lower grounded supporting substrate. A pair of circular slot resonators is embedded on the dipole-shaped metal strips in vertical polarization. Four resistors with a relatively optimal value of 100 Ohms are symmetrically assigned to connect these circular dipole-shaped metal strips together to achieve dual-polarized, and wide impedance match between the absorber with the free space further to obtain wide absorption bandwidth. The theory to realize the wideband absorption and the notch band with high notch-band-edge selectivity was explained thoroughly in our previous work [27] in detail. The supporting substrate used in the design is commercial F4B substrate with a thickness of 1 mm, a relative permittivity of 2.5, and a dielectric loss tangent of tan δ =0.002. The dimensions of rectangles for commercial lumped resistors packaging are with 0.4 mm length and 0.2 mm width. For convenient description, it is specified that at the vertical polarization, the electric field is in the direction of the *y*-axis, while the electric field in the direction of the *x*-axis is horizontal polarization.

As investigated in [27], the frequencies of the notch band can be flexibly controlled by modifying the dimensions of the metallic rectangular strip array in the lower grounded layer and circular slot resonators in the upper layer. Here, we make the frequencies of the notch band locating at X-band. Fig. 2 presents the reflection coefficients of the proposed band-notched absorber under normal and oblique incidences in vertical and horizontal polarization. It is observed that the proposed absorber shows a high notch-band-edge selectivity in vertical polarization and a wideband absorption performance in horizontal polarization simultaneously. In addition, the proposed unit cell shows stable reflection response in both vertical and horizontal polarization when illuminated with TE and TM waves incident at oblique angles up to 30 deg, as shown in Fig.2.

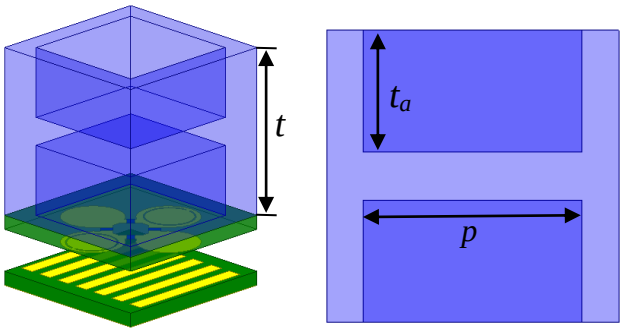

Fig. 3. Geometries of the proposed unit cell. (a). Perspective view. (b). Side view of the dielectric lens unit.

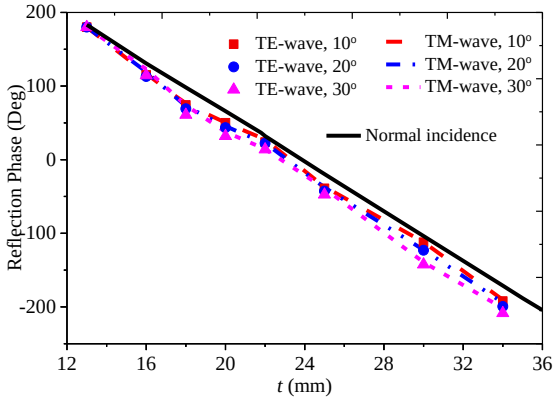

Fig. 4. Reflection phase of the UC versus *t* at 10GHz under normal and TE/TM-wave oblique incidence.

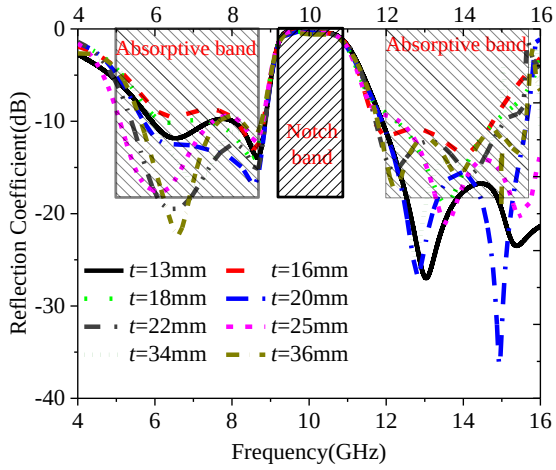

Fig.5. Reflection coefficients of the UC in vertical polarization versus *t*.

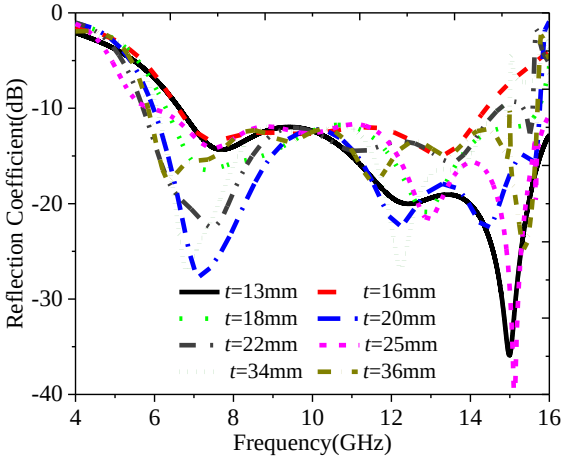

Fig. 6. Reflection coefficients of the UC in horizontal polarization versus *t*.

B. Implementation of the proposed unit cell (UC).

The proposed UC is realized by a specified dielectric lens unit coated on the previous band-notched absorber unit in subsection *A*, where the dielectric lens unit is served as a phase shift to satisfy the desired phase compensations for the proposed RA antenna design. Fig. 3 shows the geometries of the proposed

This article has been accepted for publication in a future issue of this journal, but has not been fully edited. Content may change prior to final publication. Citation information: DOI 10.1109/TAP.2019.2911342, IEEE Transactions on Antennas and Propagation

UC. The dielectric lens unit is established by using the antireflection (AR) structure as described in [30]. It is well known that the operating bandwidth of the AR structure is inherently narrow due to the presence of the quarter-wavelength air posts as the transition parts. However, when we extend and modify the AR structure to make it operate at X-band, its operating bandwidth is sufficient for our design. The values of t_a and p are determined after some optimizations, and they are equal to 4.52 mm and 9.0 mm, respectively. The material properties to establish the dielectric lens unit used here is with a thickness of t, a relative permittivity of 2.89, and a loss tangent of 0.003 at around 10GHz.

As stated before, the proposed UC should still maintain the high notch-band-edge selectivity response of the original band-notched absorber when the profile of the dielectric lens unit is varied to cover a full phase-cycle (2π) for the proposed RA antenna design. Firstly, the reflection phase of the proposed UC is examined under the different thickness of t at 10 GHz as shown in Fig. 4. It is observed that the reflection phase of the UC can absolutely cover 360 deg when the thickness t is continuously varied from 13 mm to 36 mm under the normal incidence. The linear relation between the reflection phase and thickness t can also be extended to t < 13 mm and t > 36 mm. However, the thickness t is restricted by the value of t_a that t must be large than 2* t_a. On the other hand, the thickness t is also constrained by our available 3-D printed technology process. If the thickness t were too small, it would be very hard to ensure the desired performance of the dielectric lens unit. Therefore, the thickness t from 13 to 36 mm is determined to cover a full phase-cycle and good manufacture as well. The profile of the proposed dielectric lens would be promising to be further reduced if the relative permittivity of material for the proposed dielectric lens manufacture is higher. Our available material for the proposed dielectric lens manufacture is with a relative permittivity of around 2.89.

In addition, the reflection phases of the proposed UC are also evaluated under transverse electric (TE) and transverse magnetic (TM) wave oblique incidences. From Fig. 4, it is seen that a relatively stable relationship between the reflection phase and t is obtained when the oblique incidence angle reaches up to 30°. The reflection phase differences under normal and different oblique incidences would deteriorate the aperture efficiency of the entire RA antenna.

Once the full phase-cycle property of the proposed UC is satisfied, the responses of the reflection coefficient of the proposed UC are also checked under these different thicknesses. For brevity, some discrete thicknesses (e.g., t=13mm, t=16mm, t=18mm, t=20mm, t=22mm, t=25mm, t=34mm, t=36mm) are selected to observe the reflection coefficients of the proposed UC. Fig. 5 and 6 present the reflection coefficients of the UC in vertical and horizontal polarization under these different thicknesses, respectively. Like the previous band-notch absorber, there still exists two absorption bands out of the notch band. It is also observed that the reflection amplitudes of the notch band are almost kept unchanged and can be served as a full reflectance. Although the absorption bandwidth and absorption capability out of the notch band are deteriorated more or less, the high band-notch-edge selectivity is still maintained under different thickness t, which is very important for the proposed RA antenna design. When t is equal to 25 mm, the absorption bandwidths in lower and upper reflection band are 5 to 9 GHz, and 12 to 16 GHz, respectively. In contrast, the absorption bandwidths in lower and upper reflection band are reduced to 5 to 9 GHz, and 12 to 16 GHz, respectively, when t is equal to 16 mm. Even though, an average fractional bandwidth of 45 % and 30.8 % for lower and upper reflection band with an absorptivity of more than 90 % is obtained, respectively. In addition, the wide absorption bandwidth approximately from 6 to 14 GHz with a fractional bandwidth of 80% is also observed under these different thicknesses in horizontal polarization. The amplitude and phase responses of reflection coefficients of the proposed UC ensure it a good candidate to implement an RA antenna with bandpass-like gain filtering and low-RCS properties.

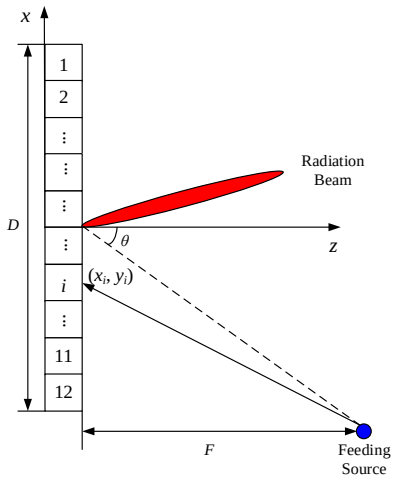

Fig. 7. The generalized mechanism of an RA antenna.

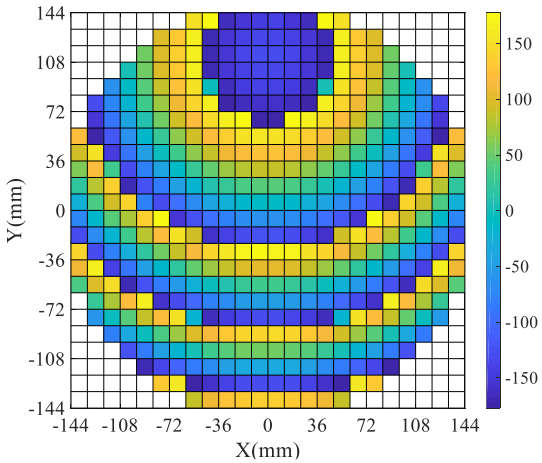

Fig. 8. The desired phase compensations on the aperture of the RA antenna at 10GHz.

This article has been accepted for publication in a future issue of this journal, but has not been fully edited. Content may change prior to final publication. Citation information: DOI 10.1109/TAP.2019.2911342, IEEE Transactions on Antennas and Propagation

III. Reflectarray Antenna Designed With the Proposed Unit Cell

In this section, the proposed UCs described in section II are fully utilized to construct an RA antenna with gain filtering and low-RCS properties for linearly-polarized source application. The dimension of the proposed RA antenna is with a diameter D=288mm (24 elements × 24 elements). A linearly-polarized Qadri- rigid horn antenna is used as the feeding source, and is oriented toward the geometrical center of the RA aperture. To avoid the shadow effects of the centrally-fed RA antenna for radiation patterns, the offset-fed method is adopted in our design. The generalized mechanism of an RA antenna is illustrated in Fig. 7. The feeding source position is usually characterized by two geometric parameters: the offset angle θ and the length F. In addition, the focal-length-to-diameter (F/D) ratio and the offset angle θ are critical for the RA antenna design to obtain good radiation performance and optimal aperture efficiency [31]. However, in the actual case, the aperture efficiency is also closely related to phase errors, feed blockage, and loss from other sources, which means the measured aperture efficiency is lower than the optimal value. After some optimizations, the feeding source is tilted by 22° and is away from the RA aperture 168 mm.

It is well known that the phase compensation of every UC is very important to achieve high gain and pencil-beam radiation patterns in a specified direction for RA antennas design. Considering the coordinate system as shown in Fig. 7, if the RA antenna is required to produce a focused beam at broadside ((0°,0°)), the desired phase compensation $\phi_R(x_i,y_i)$ at element i is given by:

$$\phi_R\left(x_i, y_i\right) = k_0 d_i \tag{1}$$

where k_0 is the propagation constant in a vacuum, and (x_i, y_i) the coordinates of element i. d_i is the distance from the phase center of the feeding source to the element i.

Based on the Eq. (1), the phase distributions on the aperture of the RA antenna at 10GHz are calculated and plotted as shown in Fig. 8. Once the desired phase compensation at every UC is obtained, the thickness of every dielectric lens unit is easily deduced accordingly. The final model of the proposed RA antenna is therefore established, and its radiation patterns and gain performance are evaluated and simulated.

IV. Fabrication, Measurement, and Discussion

In order to validate the effectiveness of the proposed UC for RA antenna to achieve bandpass-like gain filtering and low-RCS properties, the proposed RA antenna described in section III is fabricated, and its radiation patterns, realized gains, and monostatic RCS are all measured to evaluate its performance. The band-notched absorber and dielectric lens are fabricated by our available standard printed circuit board and 3-D printed technologies, respectively.

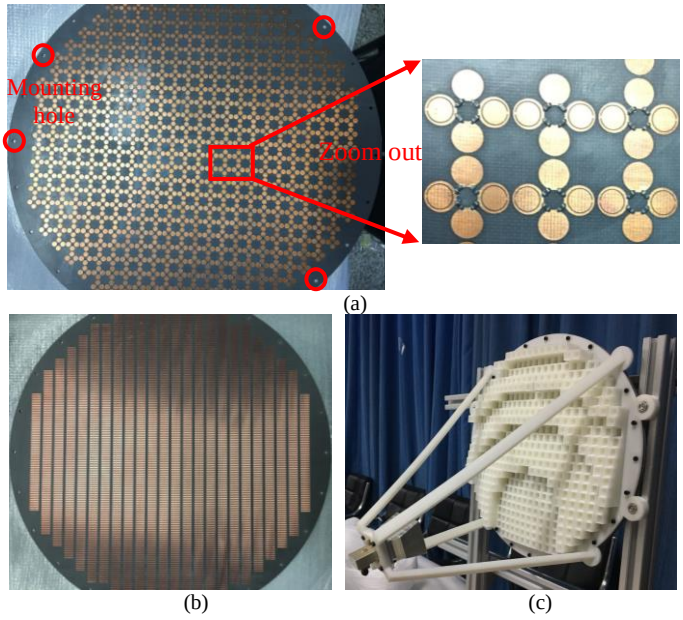

Fig. 9. Photographs of the proposed RA antenna. (a). Front view of the upper layer, (b). Front view of the lower layer, (c). Perspective view of the proposed RA antenna.

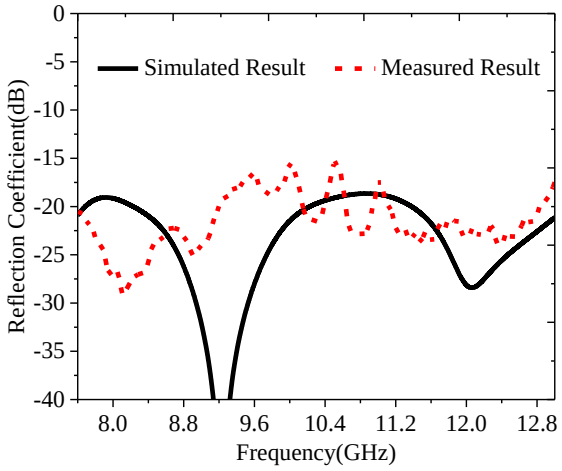

Fig.10. Comparisons of measured and simulated reflection coefficients of the proposed RA antenna.

A. Fabricated prototype and reflection coefficient measurement.

Fig. 9 shows the photographs of the fabricated band-notched absorber, dielectric lens, and the proposed RA antenna. There are 24 mounting holes around the peripheries of the lower and upper layers as shown in Fig. 9(a)-(b) to fix the lower and upper layers by using plastic screws. The separation between the lower and upper layers is determined with plastic pads with a thickness of 1mm. The commercial lumped resistors with 0402 packaging are soldered on the upper layer by using mechanical welding technique.

For simplicity and accuracy to fix the feeding source, we also use the 3-D printed technology to print a dielectric holder to fix it, and the dielectric holder is printed with the dielectric lens together as shown in Fig. 9(c), which is good for the easy

This article has been accepted for publication in a future issue of this journal, but has not been fully edited. Content may change prior to final publication. Citation information: DOI 10.1109/TAP.2019.2911342, IEEE Transactions on Antennas and Propagation

measurement of E- and H-plane radiation patterns for the proposed RA antenna. A horn antenna with a rectangular aperture is adopted to be served as the required feeding source. A probe-to-waveguide converter is used to excite the feeding source.

The reflection coefficient of the proposed RA antenna was measured with Agilent vector network analyzer (N5244A) as shown in Fig. 10, where the simulated counterpart is also plotted for comparison. It is observed that the amplitude of the measured and simulated reflection coefficients are all below -15dB over 7.6 to 13GHz. The discrepancies between the measured and simulated results are partly caused by the probe-to-waveguide converter employed in the practical measurement to excite the feeding horn antenna, and partly attributed to the manufacture errors of the feeding horn antenna. Fortunately, the discrepancies do not influence the performance of the proposed RA antenna.

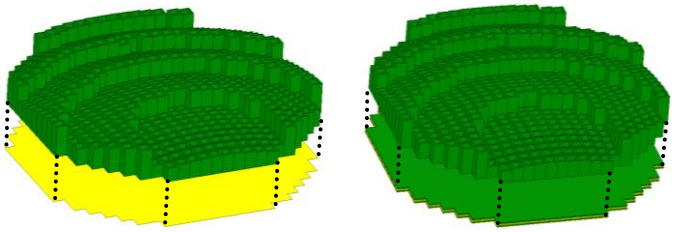

Fig. 11. Schematics of RA antennas (the feeding source is removed). (a). Conventional RA antenna, (b). Proposed RA antenna.

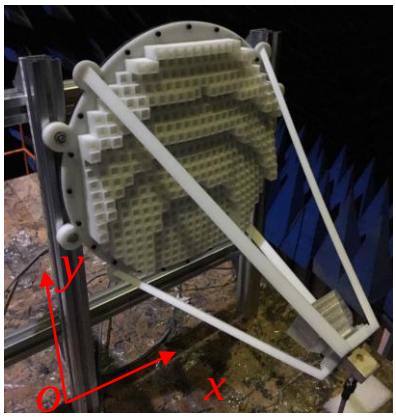

Fig.12. Measurement setup and environment.

B. Realized gain and radiation pattern measurement

In order to demonstrate the bandpass-like gain filtering performance of the proposed RA antenna, its realized gains at broadside are measured from 8.0 to 12.4 GHz, where the counterparts of a conventional RA antenna are also measured for comparison. The conventional RA antenna used here is just implemented by replacing the band-notched absorber of the proposed RA antenna with a metallic plane as shown in Fig. 11. All measurements are carried out in our anechoic chamber. The measurement setup and environment are shown in Fig. 12. The electric field radiating from the source antenna is *y*-polarized.

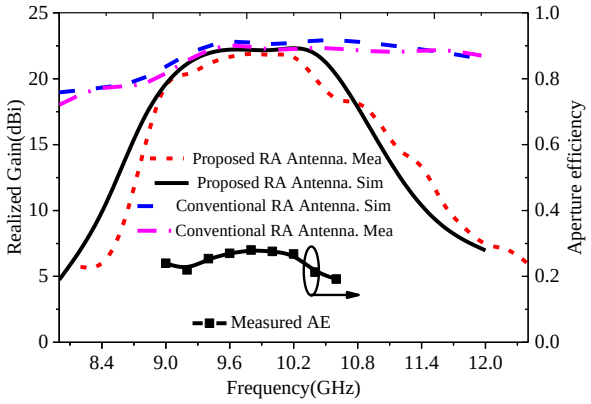

Fig. 13. Comparisons of measured and simulated realized gains at broadside over 8.0 to 12.4 GHz.

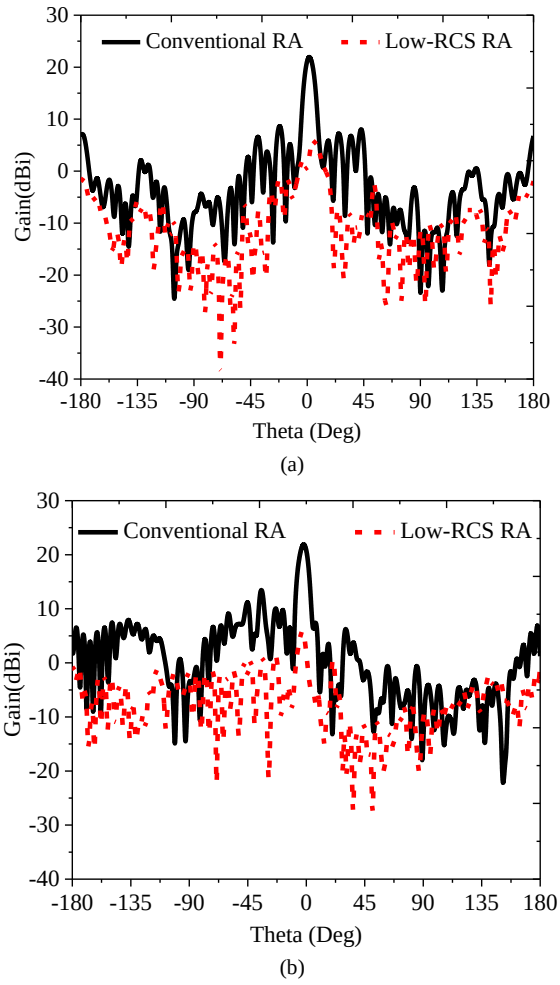

Fig. 14. The measured co-polarization of the conventional and proposed RA antennas at 12.0 GHz in (a) E-plane, and (b) H-plane.

The discrepancies between the simulated and measured realized gains are attributed to the following reasons: i). the unavoidable measurement tolerances; ii). the uncertain and inaccurate dielectric properties of the used supporting F4B substrate and the dielectric lens; iii). the machining accuracy for the dielectric lens unit. In addition, the aperture efficiencies (AE)

This article has been accepted for publication in a future issue of this journal, but has not been fully edited. Content may change prior to final publication. Citation information: DOI 10.1109/TAP.2019.2911342, IEEE Transactions on Antennas and Propagation

of the proposed RA antenna from 9.0 to 12.6 GHz are also calculated based on the measured gains and the area of the RA aperture as plotted in Fig. 13. It is observed that the measured AE of the proposed RA antenna is over 20 % from 9.0 to 12.6 GHz. It should be noted that the AE of the proposed RA antenna is promising to be further improved by using low loss tangent material for dielectric lens fabrication.

The measured boresight realized gains of the proposed and conventional RA antennas are presented in Fig.13, where the simulated realized gains are also plotted for comparison. The measured results are in great agreement with that of simulation. By comparing the realized gains of the conventional RA antenna, it is obviously found that the proposed RA antenna owes a bandpass-like gain filtering that high gains are observed within the notch band, while a sharp gain drop-off is also obtained out of the notch band. The phenomenon is reasonable as the proposed RA antenna shows an absorption performance out of the notch band. Specifically speaking, the most part of electromagnetic wave impinging from the free space is directly absorbed by the RA aperture, not scattered by the RA aperture and received by the feeding source out of the notch band. In order to verify the statement, the radiation patterns of the conventional and proposed RA antennas out of the notch band are evaluated. For brevity, the measured co-polarization of the conventional and proposed RA antennas in E- and H-plane at 12.0 GHz are compared as shown in Fig. 14. It is seen that the conventional RA antenna shows pencil-beam radiation patterns at 12.0 GHz as expected. However, the radiation patterns of the proposed RA antenna seem disturbed at 12.0 GHz. The electric field level distributions of the proposed RA antenna with θ from -180 to 180 deg are much lower than the counterparts of the conventional RA antenna, which means the total received power of the conventional RA antenna is much higher than the counterparts of the proposed RA antenna.

In order to validate the pencil-beam radiation patterns of the RA antenna within the notch band, the normalized radiation patterns of the proposed RA antenna are measured at 9.6 GHz, 10 GHz, and 10.6 GHz, respectively. The measured results are shown in Fig. 15, where the simulated counterparts are also plotted for comparisons at these frequencies. From the comparison results, it is observed that the normalized radiation patterns of co-polarization in E- (*yoz*-plane) and H-plane (*xoz*-plane) of the proposed RA antenna at 9.6, 10, and 10.6 GHz are all pencil-beam, and the normalized sidelobes below -10 dB at 9.6, 10, and 10.6 GHz are also obtained. The measured and simulated main beams of the proposed RA antenna at these frequencies are in great agreement. Moreover, the measured normalized radiation patterns of cross-polarization at these frequencies are also consistent with that of simulations, where -30 dB normalized cross-polarization levels are all obtained at these frequencies.

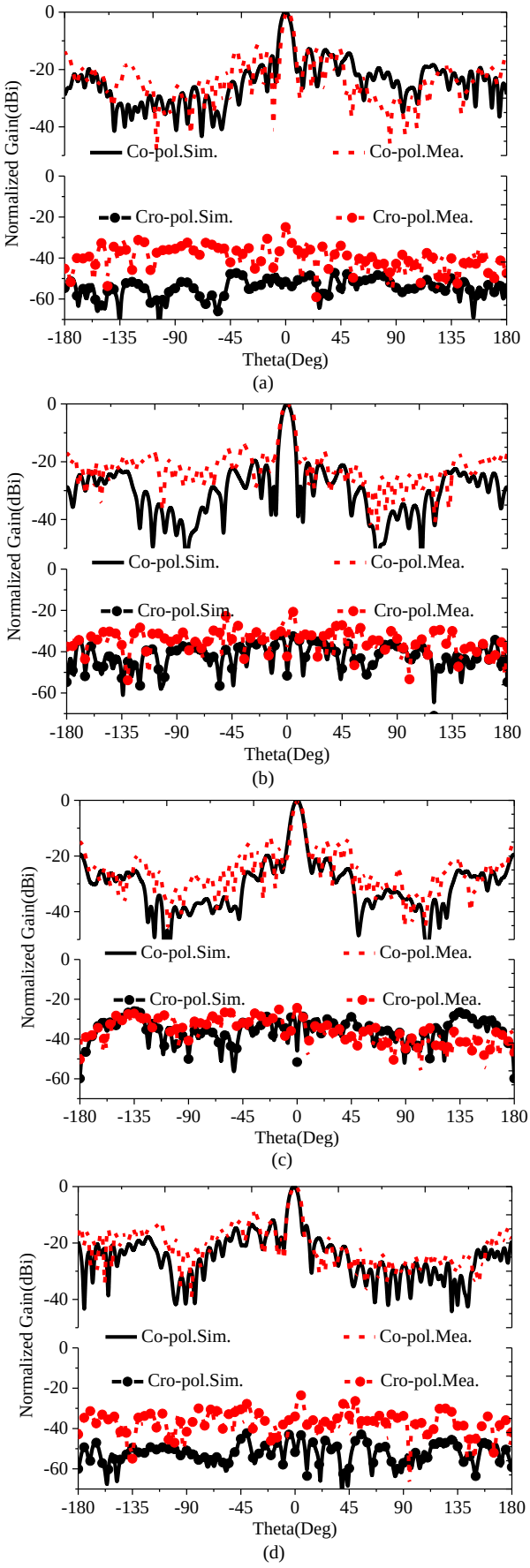

This article has been accepted for publication in a future issue of this journal, but has not been fully edited. Content may change prior to final publication. Citation information: DOI 10.1109/TAP.2019.2911342, IEEE Transactions on Antennas and Propagation

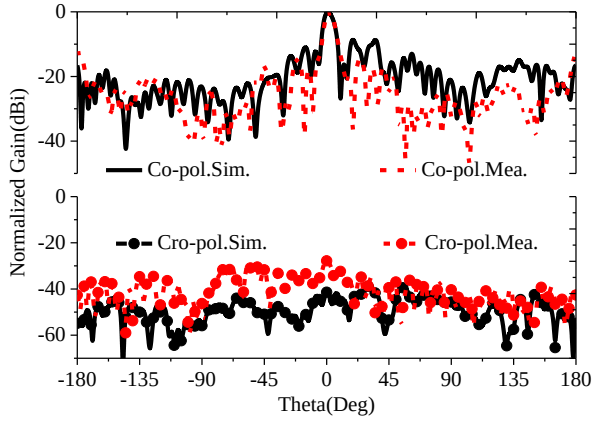

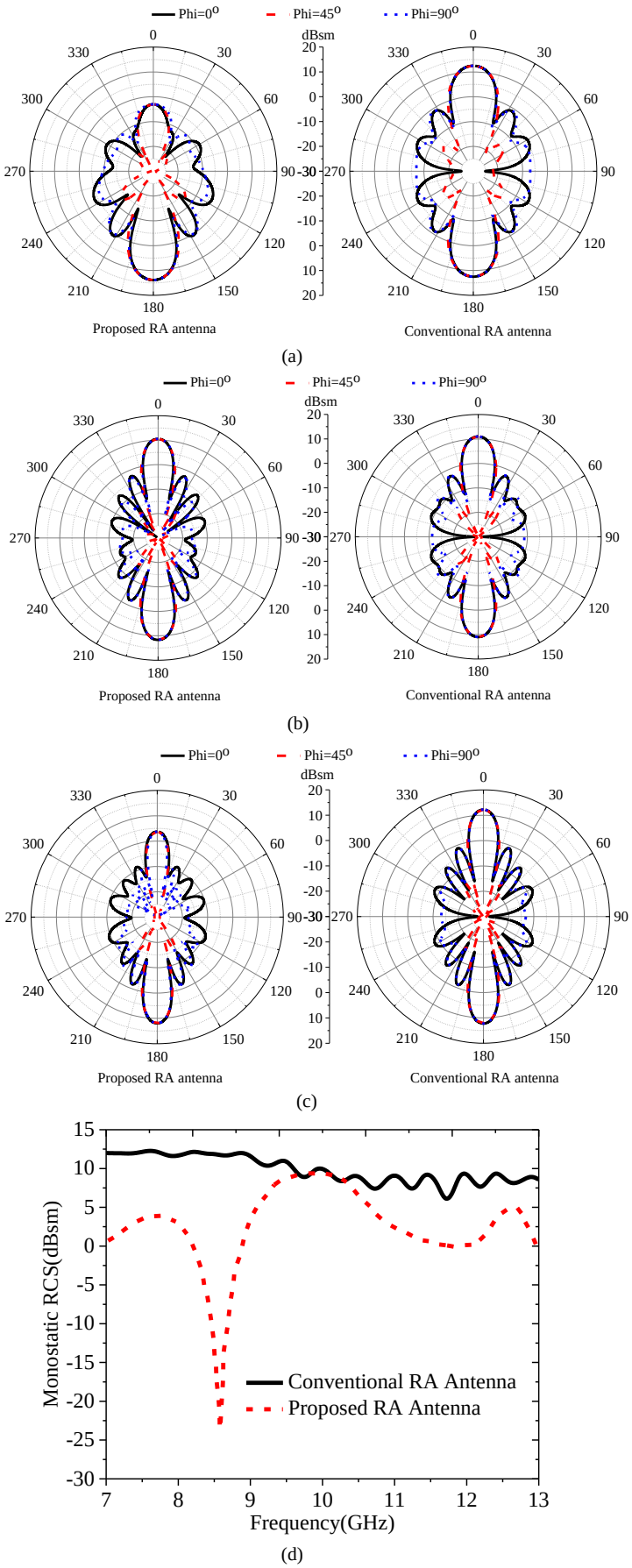

Fig. 15. Comparisons of measured and simulated normalized radiation patterns of the proposed RA antenna. (a) E-plane (*yoz*-plane) at 9.6GHz, (b) H-plane (*xoz*-plane) at 9.6GHz, (c) E-plane (*yoz*-plane) at 10.0GHz, (d) H-plane (*xoz*-plane) at 10.0GHz, (e) E-plane (*yoz*-plane) at 10.6GHz, (f) H-plane (*xoz*-plane) at 10.6GHz. (co-polarization: co-pol, cross-polarization: cro-pol.)

C. Monostatic RCS measurement

In order to validate the low RCS properties of the proposed RA antenna, the monostatic RCSs of the conventional and proposed RA antenna is measured, compared, and evaluated. First of all, the simulated bistatic scattering patterns versus theta at plane cuts of phi= 0°, 45°, and 90° of the conventional and proposed RA antennas in vertical polarization are plotted in Fig. 16 at three different frequencies of 7.0 GHz, 9.5 GHz, and 11.5 GHz. As seen from the upper half-plane of the scattering patterns, the magnitude of the scattering power for the proposed RA antenna is smaller than that of the conventional RA antenna at 7.0 and 11.5 GHz, approximately corresponds to 10 dB and 6 dB RCS reduction, respectively. The magnitude of the forward (theta = 0°) scattering power for the proposed RA antenna is almost the same as that of the conventional RA antenna at 9.5 GHz. The simulated results are consistent and reasonable as the proposed RA antenna shows RCS reduction performance out of the notch band. It is also observed the magnitudes of backward (theta = 180°) scattering power are almost the same for both conventional and proposed RA antenna due to the existence of the same PEC backplane.

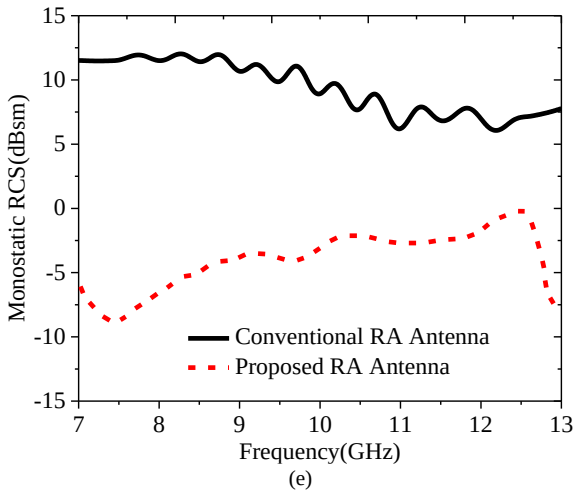

Fig. 16. Comparisons of RCS for conventional RA and proposed RA antennas. (a). simulated bistatic scattering pattern versus theta at plane cuts of phi= 0º, 45º, and 90º at 7.0 GHz in vertical polarization. (b). At 9.5 GHz. (c). At 11.5 GHz. Measured monostatic RCS for conventional and proposed RA antennas (d). In vertical polarization, and (e). In horizontal polarization.

Then, the monostatic RCS of the conventional and proposed RA antennas are also examined by measurements in our available anechoic chamber. It should be noted that both feeding sources of the RA antennas are all terminated with matching loads during the measurements. Firstly, the monostatic RCSs of the conventional and the proposed RA antennas are measured in vertical polarization corresponding to the operating polarization of the linearly-polarized feeding source. From Fig. 16 (d), it is observed that there exists a great RCS reduction out of the notch band (lower and upper bands) for the proposed RA antenna; specifically speaking, there exists about 10 dB RCS reduction from 7 to 9.2 GHz and about more than 5 dB RCS reduction from 10.5 to 13 GHz, corresponding to the bandwidth fractional of 27.16 % and 21.27 %, respectively. The monostatic RCSs of the conventional and the proposed RA antennas in horizontal polarization are then measured. It is observed in Fig. 16 (e) that a great RCS reduction from 7 to 13 GHz is also obtained with a bandwidth fractional of 60 %. The measured results validate the effectiveness of the proposed RA antenna for low RCS properties.

V. Conclusion

In conclusion, a reflectarray (RA) antenna with gain filtering and low RCS properties are proposed in the paper. The desired UC to construct the proposed RA antenna is a combination of a band-notched absorber unit and a dielectric lens unit with a specific shape, where the band-notched absorber provides a high notch- band-edge selectivity and the dielectric lens unit is employed to cover a full phase-cycle (2π). It is found that when the profile of the dielectric lens unit is varied to obtain the desired phase compensations, the high notch-band-edge selectivity of the proposed UC is still maintained. The proposed RA antenna is then constructed with these UCs. The simulated results reveal that the proposed RA antenna has a bandpass-like gain filtering performance; and within the notch band, the radiation patterns of the proposed RA antenna are pencil-beams, which are all experimentally verified by the measured results.

In addition, the monostatic RCSs of the proposed RA antenna are measured and evaluated, where the counterparts of a conventional RA antenna that the band-notched absorber of the proposed RA antenna is replaced by a metallic plane is also measured. The measured results show that a great RCS reduction is observed out of the notch band in vertical polarization and a wideband RCS reduction is also obtained in horizontal polarization for the proposed RA antenna. The measured results validate the effectiveness of the proposed RA antenna for low RCS property.

ACKNOWLEDGMENT

The authors would like to express their great thanks to Prof. S. W. Qu from University of Electronic Science and Technology of China for providing the feeding source. Also, the insightful and constructive comments from the anonymous reviewers are highly appreciated.

References

[1] J. Huang, and J. A. Encinar, *Reflectarray Antennas*. Hoboken, NJ, USA: Wiley, 2008.

[2] J. Shaker, M. R. Chaharmir, and J. Ethier, *Reflectarray Antennas: Analysis, Design, Fabrication, and Measurement*. Norwood, MA, USA: Artech House, 2014.

[3] C. Han, J. Huang, and K. Chang, "A high efficiency offset-fed X/Ka-dual-band reflectarray using thin membrances," *IEEE Trans. Antennas Propag*., vol. 53, no. 9, pp. 2792-2797, Sep 2005.

[4] S. Hsu, C. Han, J. Huang, and K. Chang, "An offset linear-array-fed Ku/Ka dual-band reflectarray for planet cloud/Precipitation radar," *IEEE Trans. Antennas Propag*., vol. 55, no. 11, pp. 3114-3122, Nov 2007.

[5] M. Alsath, M. Kanagasabai, and S. Arunjumar, "Dual-band dielectric resonator reflectarray for C/X-bands," *IEEE Antennas Wireless Propag. Lett*, vol. 11, pp. 1253-1256, 2012.

[6] B. You, Y. Lu, J. Zhou, and H. Chou, "Numerical synthesis of dual-band reflectarray antenna for optimum near-field radiation," *IEEE Antennas Wireless Propag. Lett*, vol. 11, pp. 760-762, 2012.

[7] Z. Zarghani, and Z. Atlasbaf, "A new broadband single-layer dual-band reflectarray antenna in X- and Ku-bands," *IEEE Antennas Wireless Propag. Lett*, vol. 14, pp. 602-605, 2012.

[8] R. Deng, S. Xu, F. Yang, and M. Li, "Single-layer dual-band reflectarray antennas with wide frequency ratios and high aperture efficiencies using phoenix elements," *IEEE Trans. Antennas Propag*., vol. 65, no. 2, pp. 612-622, Feb 2017.

[9] M. Albooyeh, N. Komjani, and M. Mahani, "A circularly polarized element for reflectarray antennas," *IEEE Antennas Wireless Propag. Lett*, vol. 8, pp. 319-322, 2009.

[10] R. Malfajjani, Z. Atlasbaf, "Design and implementation of a broadband single layer circularly polarized reflectarray antenna," *IEEE Antennas Wireless Propag. Lett*, vol. 11, pp. 973-976, 2012.

[11] T. Smith, U.Gothelf, O. Kim, and O. Breinbjerg, "Design, manufacturing, and testing of a 20/30-GHz dual-band circularly polarized reflectarray antenna," *IEEE Antennas Wireless Propag. Lett*, vol. 12, pp. 1480-1483, 2013.

[12] T. Smith, U. Gothelf, O. Kim, and O. Breinbjerg, "An FSS-backed 20/30 GHz circularly polarized reflectarray for a shared aperture L- and Ka-band satellite communication antenna," *IEEE Trans. Antennas Propag*., vol. 62, no. 2, pp. 661-668, Feb 2014.

[13] Q. Gao, J. Wang, Y. Li, and Z. Li, "A multiresonant element for bandwidth enhancement of circularly polarized reflectarray antennas," *IEEE Antennas Wireless Propag. Lett*, vol. 17, pp. 727-730, May 2018.

[14] H. Kamoda, T. Iwasaki, J. Tsumochi, T. Kuki, and O. Hashimoto, "60-GHz electronically reconfigurable large reflectarray using single-bit phase shifters," *IEEE Trans. Antennas Propag*., vol. 59, no. 7, pp. 2524-2531, Jul. 2011.

[15] R. Pereira, R. Gillard, R. Sauleau, P. Potier, T. Dousset, and X. Delestre, "Dual linearly-polarized unit cells with nearly 2-bit resolution for reflectarray applications in X-band," *IEEE Trans. Antennas Propag*., vol. 60, no. 12, pp. 6042-6048, Dec. 2012.

[16] E. Carrasco, M. Barba, and J. A. Encinar, "X-band reflectarray antenna with switching-beam using PIN diodes and gathered elements," *IEEE Trans. Antennas Propag*., vol. 60, no. 12, pp. 5700-5708, Dec. 2012.

[17] X. Yang, S. Xu, F. Yang, M. Li, Y. Hou, S. Jiang, and L. Liu, "A broadband high-efficiency reconfigurable reflectarray antenna using mechanically rotation elements," *IEEE Trans. Antennas Propag*., vol. 65, no. 8, pp. 3959-3966, Aug. 2017.

[18] W. An, S. Xu, F. Yang, and J. Gao, "A ka-band reflectarray antenna integrated with solar cells," *IEEE Trans. Antennas Propag*., vol. 62, no. 11, pp. 5539-5546, Nov. 2014.

[19] M. Moharram, and A. Kishk, "Optically transparent reflectarray antenna design integrated with solar cells," *IEEE Trans. Antennas Propag*., vol. 64, no. 5, pp. 1700-1712, May. 2016.

[20] S. Shynu, M. Ons, P. McEvoy, M. Ammann, S. McCormack, and B. Norton, "Integration of microstrip patch antenna with polycrystalline silicon solar cell," *IEEE Trans. Antennas Propag*., vol. 57, no. 12, pp. 3969-3972, Dec. 2009.

[21] E. Lim, L. Leung, C. Su, and H. Wong, "Green antenna for solar energy collection," *IEEE Antennas Wireless Propag. Lett*, vol. 9, pp. 689-692, 2010.

[22] M. Tanaka, R. Suzuki, Y. Suzuki, and J. Kirchhof, "Microstrip antenna with solar cells for microsatellites," *in Proc. Antennas Propag. Soc. Int. Symp. (AP-S) Dig*., vol. 2, pp. 786-789, 1994.

[23] M. Rafaei-Booket, Z. Atlasbaf, and M. Shahabadi, "Broadband reflectarray antenna on a periodically perforated substrate," *IEEE Trans. Antennas Propag*., vol. 64, no. 8, pp. 3711-3717, Aug. 2016.

[24] W. Li, S. Gao, L. Zhang, Q. Luo, and Y. Cai, "An untra-wide-band tightly coupled dipole reflectarray antenna," *IEEE Trans. Antennas Propag*., vol. 66, no. 2, pp. 533-540, Feb. 2018.

[25] P. Nayeri, M. Liang, R. Sabory-Garcia, M. Tuo, F. Yang, M. Gehm, H. Xin, and A. Elsherbeni, "3D printed dielectric reflectarrays: low-cost high-gain antennas at sub-millimeter waves," *IEEE Trans. Antennas Propag*., vol. 62, no. 4, pp. 2000-2008, Apr. 2014.

[26] R. Deng, F. Yang, S. Xu, and M. Li, "A 100-GHz metal-only reflectarray for high-gain antenna application," *IEEE Antennas Wireless Propag. Lett*, vol. 15, pp. 178-181, 2016.

[27] P. Mei, X. Lin, J. Yu, and P. Zhang, "A band-notched absorber designed with high notch-band-edge selectivity," *IEEE Trans. Antennas Propag*., vol. 60, no. 12, pp. 5700-5708, Jul. 2017.

[28] P. Mei, *et al*., "Development of a low radar cross section antenna with band-notched absorber," *IEEE Trans. Antennas Propag*., vol. 60, no. 12, pp. 5700-5708, Feb. 2018.

[29] H. Huang, and Z. Shen, "Low-RCS reflectarray with phase controllable absorptive frequency –selective reflector," *IEEE Trans. Antennas Propag*, vol. 67, no. 1, pp. 190-198, Jan 2019.

[30] H. Yi, S. Qu, K. Ng, C. Chan, and X. Bai, "3-D printed millimeter-wave and terahertz lenses with fixed and frequency scanned beam," *IEEE Trans. Antennas Propag*., vol. 64, no.2, pp. 442-449, Feb. 2016.

[31] A. Yu, F. Yang, A. Elsherbeni, J. Huang, and Y. Rahmat-Samii, "Aperture efficiency analysis of reflectarray antennas," *Microw Opt Tech Lett*., vol. 52, no. 2, pp. 364-372. Feb 2010.

Peng Mei (S'15) was born in Suizhou, Hubei province, China, in 1993. He received the B.Sc. and M. Sc. degree (with highest honors) in electromagnetic field and microwave technology from the University of Electronic and Science Technology of China (UESTC), Chengdu, China, in 2015 and 2018, respectively. He is currently pursuing his Ph.D degree with the Antennas, Propagation and Millimeter-wave Systems section, Department of Electronic Systems, Aalborg University, Aalborg, Denmark. Mr. Mei was awarded the Outstanding Student of UESTC (only 10 awardee every year of UESTC) in 2017, was awarded Excellent Graduate Student of UESTC in 2018, and was also awarded Excellent Graduate Student of Sichuan Province in 2018. His current research interests involve: periodic structures, metamaterial absorbers, low radar cross section (RCS) antennas, Reflectarray/Transmitarray antennas, and multibeam millimeter-wave antennas.

Shuai Zhang (SM'18) received the B.E. degree from the University of Electronic Science and Technology of China (UESTC), Chengdu, China, in 2007 and the Ph.D. degree in electromagnetic engineering from the Royal Institute of Technology (KTH), Stockholm, Sweden, in 2013. After his Ph.D. studies, he was a Research Fellow at KTH. In April 2014, he joined Aalborg University, Denmark, where he currently works as Associate Professor. In 2010 and 2011, he was a Visiting Researcher at Lund University, Sweden and at Sony Mobile Communications AB, Sweden, respectively. He was also an external antenna specialist at Bang & Olufsen, Denmark from 2016-2017. He has coauthored over 50 articles in well-reputed international journals and over 16 (US or WO) patents. His current research interests include: mobile terminal mmwave antennas, biological effects, CubeSat antennas, Massive MIMO antenna arrays, UWB wind turbine blade deflection sensing, and RFID antennas.

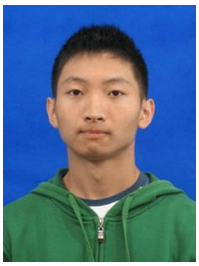

Yang Cai was born in Sichuan, China, in 1995. He received his B.Sc. degree in electromagnetic field and wireless technology from University of Electronic Science and Technology of China (UESTC), Chengdu, China, in 2018. He is currently pursuing his M.S. degree in electromagnetic field and microwave technology at UESTC. His current research interests include periodic structures, metamaterial absorbers, and low radar cross section (RCS) reflectarray antenna.

Xian Qi Lin (M'08-SM'15) was born in Zhejiang Province, China, on July 9, 1980. He received the B. Sc. degree in electronic engineering from the University of Electronic Science and Technology of China (UESTC), Chengdu, China, in 2003, and the Ph.D. degree in electromagnetic field and microwave technology from Southeast University, Nanjing, China, in 2008. He joined the Department of Microwave Engineering, UESTC, in August, and became an Associate Professor and a Doctoral Supervisor in July 2009 and

December 2011, respectively. From September 2011 to September 2012, he was a Postdoctoral Researcher in the Department of Electromagnetic Engineering, Royal Institute of Technology (KTH), Stockholm, Sweden. He is currently a Full Professor at UESTC. He has authored more than ten patents, more than 40 scientific journal papers, and has presented more than 20 conference papers. His research interests include microwave/ millimeter-wave circuits, metamaterials, wireless power transfer, energy harvesting, and antennas.

Gert Frølund Pedersen was born in 1965. He received the B.Sc. and E.E. (Hons.) degrees in electrical engineering from the College of Technology in Dublin, Dublin Institute of Technology, Dublin, Ireland, in 1991, and the M.Sc.E.E. and Ph.D. degrees from Aalborg University, Aalborg, Denmark, in 1993 and 2003, respectively. Since 1993, he has been with Aalborg University where he is a Full Professor heading the Antennas, Propagation and Millimeter-wave Systems LAB with 25 researchers. He is also the Head of the Doctoral School on wireless communication with some 40 Ph.D. students enrolled. His research interests include radio communication for mobile terminals especially small antennas, diversity systems, propagation, and biological effects. He has published more than 500 peer reviewed papers, 6 books, 12 book chapters and holds over 50 patents. He has also worked as a Consultant for developments of more than 100 antennas for mobile terminals including the first internal antenna for mobile phones in 1994 with lowest SAR, first internal triple-band antenna in 1998 with low SAR and high TRP and TIS, and lately various multiantenna systems rated as the most efficient on the market. He has worked most of the time with joint university and industry projects and have received more than 21 M$ in direct research funding. He is currently the Project Leader of the RANGE project with a total budget of over 8 M$ investigating high performance centimeter/ millimeter-wave antennas for 5G mobile phones. He has been one of the pioneers in establishing over-the-air measurement systems. The measurement technique is now well established for mobile terminals with single antennas and he was chairing the various COST groups with liaison to 3GPP and CTIA for over-the-air test of MIMO terminals. He is currently involved in MIMO OTA measurement.